

## Evaluation of eco-friendly concrete having waste PET as fine aggregates

Gideon O. Bamigboye<sup>a,\*</sup>, Karnik Tarverdi<sup>b</sup>, Amarachi Umoren<sup>a</sup>, Daniel E. Bassey<sup>a</sup>,  
Uchekukwu Okorie<sup>c</sup>, Joel Adediran<sup>a</sup>

<sup>a</sup> Department of Civil Engineering, Covenant University, Ota, Ogun State, Nigeria

<sup>b</sup> Department of Chemical Engineering, Brunel University, London, United Kingdom

<sup>c</sup> Department of Economics, Covenant University, Ota, Ogun State, Nigeria



### ARTICLE INFO

#### Keywords:

Construction materials  
Compressive strength  
Fine aggregates  
Concrete  
Polyethylene terephthalate  
Cement

### ABSTRACT

This study assesses the impacts of recycling waste polyethylene terephthalate (PET) plastic bottles as a partial substitute for fine natural aggregates on the workability, mechanical, microstructural, economic, and thermal properties of concrete. The mix design adopts a concrete mix ratio of 1:2:4 for grade M25, 0.55 water/cement ratio, ordinary Portland cement (OPC) as the binder, varying proportions of heat-processed waste PET and river sand as fine aggregates, and granite as coarse aggregate. Results indicate that workability increased with increasing percentages of waste PET plastics until the 40%PET level, beyond which workability reduces. Compressive and split tensile strength decreased with increasing percentages of waste PET plastics. However, 10% to 40%-PET-modified mixes achieved the recommended strength for M20 concrete. Microstructural analysis on the 30%PET indicates higher quantities of O and Ca, and trivial percentages of Mg, Si, C, Al, and Au. Whereas 100%PET indicates the presence of only C, O, and Au. 100%PET endures three transition stages during heat flow. A glass transition, an exothermic peak below decomposition temperature during cooling at a temperature of 199.88 °C from PET crystallization, and a baseline shift after the endothermic peak at 243.22 °C. Thermogravimetry revealed that 100%PET suffers a dual-stage decomposition, an initial stage accounting for an 87.41% reduction in sample mass and a second stage accounting for a further mass loss of 12.79%. Highly significant statistical correlations and regressions developed variations between PET% and the workability and mechanical parameters. The study shows that heat-processed PET-modified concrete is appropriate for structural applications due to its suitable fresh, mechanical, microstructural, and thermal properties. Besides, this practice is eco-friendly and sustainable as it conserves natural resources.

### 1. Introduction

Plastic production has been on a constant rise in current years as a result of its wide range of utility in our daily lives, although the resultant wastes are considered non-biodegradable and chemically toxic, and as such, pose adverse effects on the environment (Almeshal et al., 2020; Boucedra et al., 2020). The United Nations Environment Program (UNEP) estimates the global annual production of plastics at over 400 million tonnes, of which around 87% (350 million tonnes) becomes waste plastics. As of 2015, The plastic packaging industry produced single-use plastics at an annual rate of about 141 million tonnes, which accounted for 47% of the total plastic waste production (UNEP, 2018). China is currently the world's largest producer of plastic packaging wastes in whole (40 million tonnes), while the USA leads

on a per capita basis (45 million tonnes) (UNEP, 2018). The production rate of plastics by industries worldwide is illustrated in Fig. 1.

Large quantities of single-use plastics often end up recycled, littered on streets, landfilled, indiscriminately dumped, or incinerated (Bamigboye et al., 2019). Recent evaluations indicate that 79% of the waste plastics ever generated still accrues in dumps, landfills, or the environment, while around 12% has undergone incineration, and only about 9% has been recycled (UNEP, 2018). The largest generators of poorly managed waste plastics are China, with 8.8 million tons per year (27% of global total), and Indonesia, with 3.2 million tonnes per year (10% of global total) (USEPA, 2017). Several attempts are being made to promote the recycling of plastics. For instance, a preliminary agreement was reached in 2017 between the European Parliament, European Council, and European Commission to set a milestone for

\* Corresponding author.

E-mail address: [gideon.bamigboye@covenantuniversity.edu.ng](mailto:gideon.bamigboye@covenantuniversity.edu.ng) (G.O. Bamigboye).

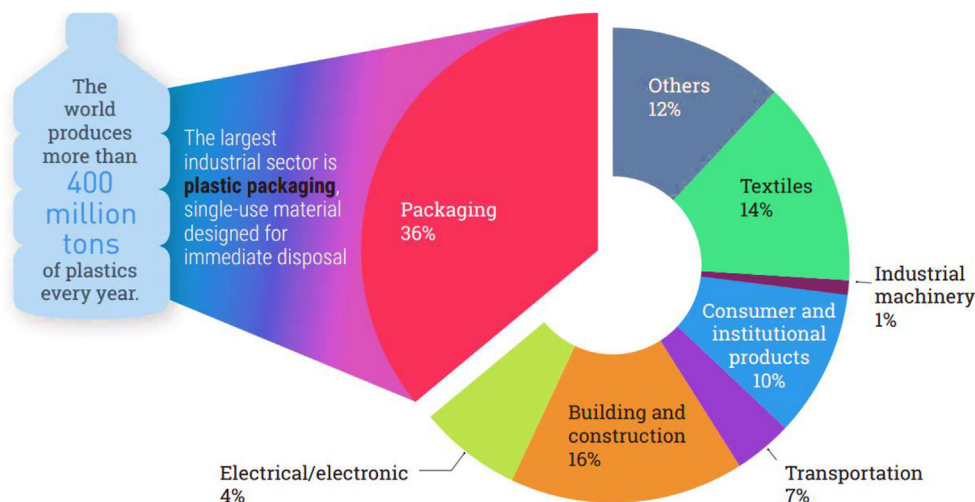


Fig. 1. Global production of plastic by industries (2015) (Source: UNEP, 2018).

plastic recycling by 2025 at 50%, to be increased by 2030 to 55% with energy recovery. It was projected that by 2050, there would be nearly 12 billion tonnes of waste plastics dumped in landfills if measures are not put in place to curtail the current plastic production, consumption, and waste management practices (UNEP, 2018). This, among other reasons, has, in the past few decades, led to a series of studies aimed at proffering methods for recycling these waste plastics in the construction industry. The two broad classes of plastics and their single-use applications are shown in Fig. 2.

Concrete is the second most utilized material after water because of its ease-of-handling and mechanical strength (Faraj et al., 2020; Saikia and De Brito, 2012). Over the years, the ever-growing rate of development and urbanization has led to excessive exploitation and depletion of natural resources used in concrete production (Bhardwaj and Kumar, 2017). These resources majorly include sand, gravel, and cement (limestone). Aggregates constitute around 65 to 80% of the concrete volume and are responsible for their strength, porosity, density, workability, and durability (Faraj et al., 2019). Substantial quantities

of fine and coarse aggregates are needed to produce large volumes of concrete worldwide annually. The utilization of waste materials in concrete can help conserve natural resources while offering a more sustainable solution to the waste disposal concerns (Babafemi et al., 2018; Spiesz et al., 2016; Tang et al., 2019).

Among the multiple recycling approaches for waste plastics, the reutilization of polyethylene terephthalate (PET) in producing composites for building and road construction is considered an ideal disposal technique (Bamigboye et al., 2020). Through this technique, waste plastics can be reused with no quality degradation during its processing while replacing the fast-depleting natural materials, supporting conservation (Almeshal et al., 2020; Maharaj et al., 2019; Perera et al., 2019). The recycling of waste plastics in cement-based composites have been widely studied. Waste plastics were utilized majorly as plastic aggregates, substituting natural aggregates. These studies have examined the fresh and hardened properties of the modified composites and recorded variations in performance, mostly typified by strength declines and improvements in workability

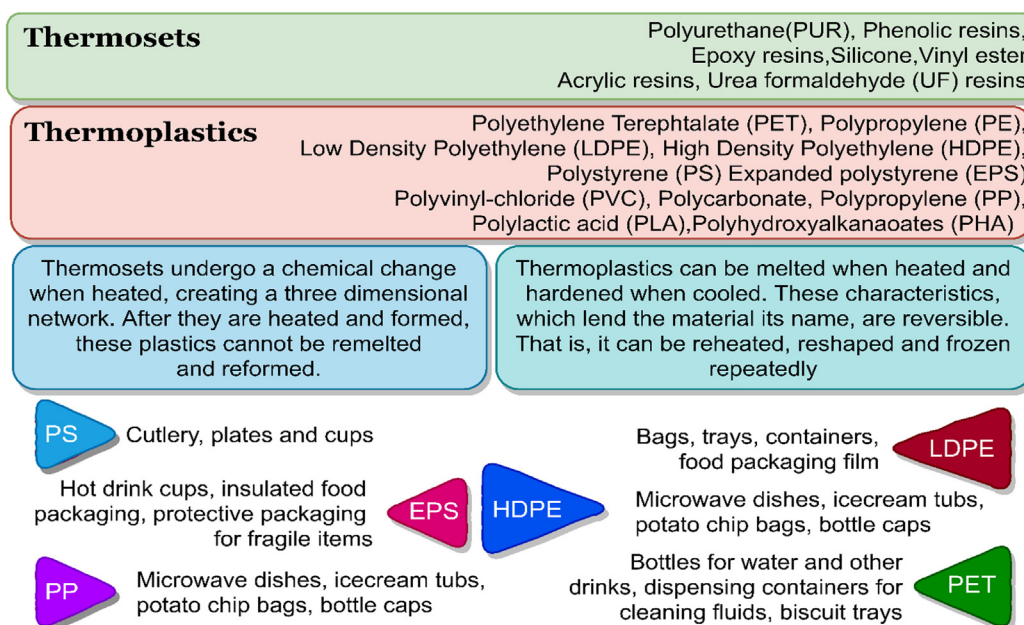


Fig. 2. Major categories and applications of plastics (Source: Li et al., 2020; UNEP, 2018).

(Islam et al., 2016; Lee et al., 2019; Maharaj et al., 2019; Mohammed and Rahim, 2020; Perera et al., 2019; Sharma and Bansal, 2016; Silva et al., 2013). The use of these waste plastics also achieves a critical goal in the construction industry by significantly reducing the density and deadweight of produced concrete, thereby mitigating earthquakes' dangers (Akçaözöğlü et al., 2010). Other benefits include improved thermal insulation, reduced initial construction costs, and reduced manufacturing and handling times (Colangelo et al., 2016).

In this context, the objective of this study is to evaluate the effects of the total or partial substitution of natural river sand by heat-processed PET plastic aggregates on the workability, mechanical, microstructural, economic, and thermal properties of cement-based concrete. It is important to note that most previous studies utilized regular PET plastic flakes as substitutes for fine natural aggregates (Needhidasan et al., 2020; Sadrmomtazi et al., 2016; Silva et al., 2013). However, this study utilizes heat pre-treated PET plastic aggregates in the replacement of fine natural aggregates. The PET treatment method was adopted from a study by Islam et al. (2016), who replaced natural coarse aggregates. No previous study has assessed the microstructure and thermal properties of PET-fine-aggregate-based concretes produced using this pre-treatment methodology.

## 2. Experimental program

### 2.1. Materials

The current study used materials sourced locally. Dangote 3X brand of OPC with Grade 42.5 N was used and hydrated with drinkable water as a binder. The physical properties and chemical composition of Dangote 3X brand grade 42.5 N are shown in Table 1. The fine aggregates used for this study were sourced from River Ogun, Abeokuta, Ogun State, Nigeria. The natural aggregate had a water absorption rate of 2.4%. The grain size distribution of all aggregates used is illustrated in Fig. 3. Shredded waste PET plastic bottles obtained from Covenant University's Waste to Wealth Centre were used in proportions as replacements for FA. The natural coarse aggregates (CA) used was sourced from the quarry located in Igbo-ora, Oyo State, with a water absorption rate of 0.486%.

### 2.2. Preparation of materials

The plastic aggregates were prepared by first cleaning off all labels, adhesives, and other visible impurities from the PET plastic bottles, then shredding into smaller particles using a plastic shredder. The shredded plastic particles were then heated and melted into a molten state using a gas stove and a steel pot. The melted plastic was then

**Table 1**

Characteristic composition of 42.5 N grade cement used (Source: An et al., 2020; Boucedra et al., 2020).

Chemical composition (%)	
Al <sub>2</sub> O <sub>3</sub>	4.44
MgO	2.32
SiO <sub>2</sub>	20.71
CaO	62.80
SO <sub>3</sub>	2.37
Fe <sub>2</sub> O <sub>3</sub>	2.78
Cl <sup>-</sup>	0.007
Na <sub>2</sub> O + K <sub>2</sub> O	0.88
f-CaO	0.79
Loss of ignition	3.38
Mineralogical composition (% by mass)	
C <sub>2</sub> S	6.98
C <sub>3</sub> S	68.84
C <sub>3</sub> A	2.58
C <sub>4</sub> AF	17.69

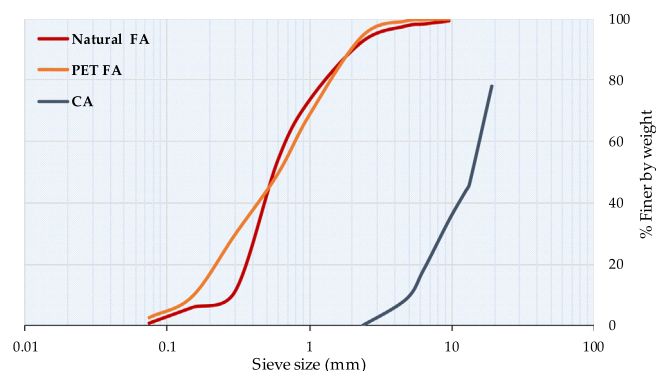


**Fig. 3.** Particle size distribution curves for aggregates.

poured into a mold and left to cool for 24 h, as shown in Fig. 4. Heating was done to ensure that the resulting plastic aggregate was homogeneous, such that it forms a coalesce after cooling. Afterwards, the plastic was broken into pieces using a mallet. These pieces were then further ground into granules using a mechanized grinder before sieving to obtain maximum sizes suitable for fine aggregate. The produced plastic aggregates gave a water absorption rate of 0.27%. The natural aggregates (fine and coarse) were as well sampled, air-dried, properly cleansed to remove impurities, and sieved.

### 2.3. Mix design and batching

In this study six sample mixes were considered. A control mix with 100 percent natural aggregates (fine and coarse) and five designed PET-modified aggregates combining river sand and PET plastic aggregates in varying percentage ratios (100:0, 90:10, 80:20, 70:30, 60:40, and 0:100), as fine aggregates. The concrete produced was cured by immersing in a curing pool filled with potable water for up to 28 days. The batching method adopted for the study is shown in Fig. 5. The mix ratio adopted for the study was 1:2:4 with a strength of target of 25 N/mm<sup>2</sup> for concrete grade M25 and a 0.55 as fixed water/binder ratio as detailed in Table 2.

### 2.4. Tests conducted

The tests performed in this research were categorized into four: the fresh concrete workability tests (to measure the consistency and fluidity of the mix), hardened concrete tests (to determine the mechanical characteristics of concrete produced), the microstructural, and the thermal conductivity tests. All the experimental tests were conducted with reference to processes, as specified in relevant standards.

#### 2.4.1 Tests on workability

The slump cone and compaction factor tests were conducted on each fresh mix batch to assess the processed PET plastic aggregates' effects on concrete's workability and consistency. These tests were performed following guidelines in ASTM C143/C143M-15a and IS1199-2-

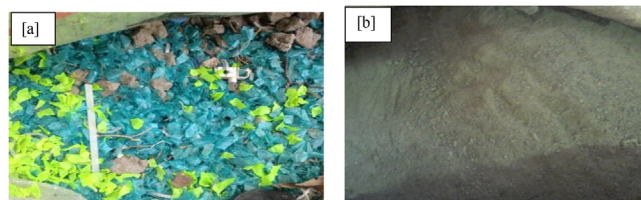


**Fig. 4.** PET plastic treatment process [a] after shredding [b] fine plastic aggregate produced.

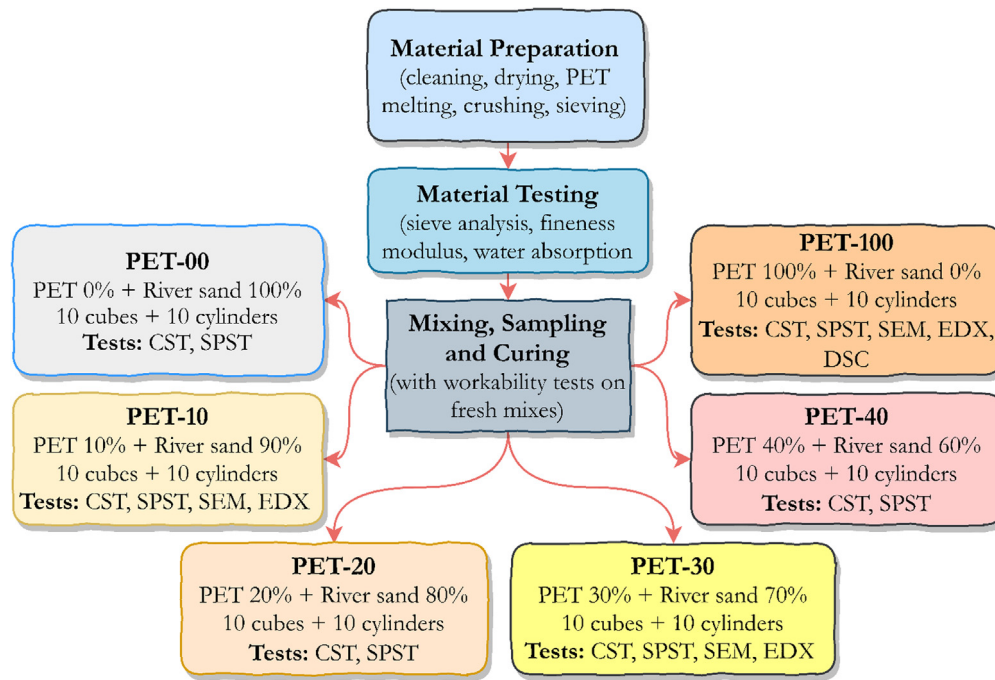


Fig. 5. Experimental program.

Table 2  
Mix design.

Concrete Batch	Content of components in kg/m <sup>3</sup>				
	Cement	Water	Natural-FA	PET-FA	Granite
PET-00	315	173.25	630	0	1260
PET-10	315	173.25	567	63	1260
PET-20	315	173.25	504	126	1260
PET-30	315	173.25	441	189	1260
PET-40	315	173.25	378	252	1260
PET-100	315	173.25	0	630	1260

2018, respectively. During the mixing of each concrete batch, a levelled surface ground was prepared, and the slump cone was placed on it. The cone was filled with concrete and tamped. To compute the slump value, the cone was then raised vertically, and the slump was calculated as the difference in height between the slump sample and the cone.

#### 2.4.2 Compressive strength test

Compressive strength tests were conducted after 3, 7, 14, and 28 days of curing. The compression testing machine (CTM) with a serial number C193A/S20UT-M was used for crushing the concrete cubes samples in line with ASTM, C39/C39M-20. The concrete samples were placed in the CTM, and the load was applied to the samples at a defined speed until failure happened. The result obtained from the crushing value for each sample was calculated using the recorded failure loads.

#### 2.4.3 Split tensile strength test

Split tensile strength tests (SPST) were conducted on all mixes after 3, 7, 14, and 28 days of curing. The tests were done following guidelines in ASTM C496/C496M-17 on the concrete cylinder samples with 200 mm × 100 mm, using a compression testing machine. Concrete samples produced were placed in the CTM horizontally and braced on the top and beneath by steel strips along the axis of its splitting. At the predefined constant rate, the load was then gradually applied

until the concrete sample split. The result for each concrete mix batch was calculated using the recorded failure loads.

#### 2.4.4 Microstructural analysis

A standard LEO 1455VP (LEO Electron Microscopy) model scanning electron microscope (SEM) was used to examine the effects of PET addition on the microstructure of the composite at 10, 30, and 100% PET plastic replacement levels. SEM generates images of the specimen in high resolution by rastering an electron beam focused on the specimen's surface and recognizing backscattered or secondary electron signals. Correspondingly, energy-dispersive X-ray spectroscopy (EDX) analyzer was used for determining the qualitative and quantitative elemental composition of the tested composites. The electron beam-specimen contact produces a range of signals containing a variety of data on the samples such as cathodoluminescence; indicating the structure of electrons and the chemical composition of the material, secondary electron; for topographic data, and transmitted electron; for a description of the internal structure and crystallography of the material as shown in Fig. 5 (Goldstein et al., 2018).

#### 2.4.5 Thermal analysis

Differential scanning calorimetric (DSC) and thermogravimetric analysis (TGA) thermal analysis were conducted on the 100%-PET-modified samples. The DSC and TGA models used were SDT Q600V8.3 Build 101, and DSC Q2000 V24.10 Build 122. The Heat-Cool-Reheat method was adopted. DSC analysis determines the

amount of thermal energy absorbed or expelled by a test sample during heating or cooling cycles. It quantitatively and qualitatively produces endothermic (heat absorption) and exothermic (heat evolution) data from thermal developments. The test sample was positioned on a pan and placed on a constantan disc on the DSC analysis cell; a chromel wafer was positioned directly underneath. The concrete sample's temperature was measured by chromel-alumel thermocouple (CAT). An empty reference pan is placed on a symmetric platform directly over a chromel wafer and CAT. The flow of heat is calculated as the difference in temperature between the test sample and the control chromel wafers as per ASTM E2160-04-2018. TGA technique was adopted to monitor the change in the sample's mass relative to temperature (Groenewoud, 2001; Jeske et al., 2012).

### 3. Result and discussions

#### 3.1. Workability tests

The compaction factor and slump tests were performed on all mixed batches to determine their consistency and workability. Slump results illustrated in Fig. 6 show a continuous increase in workability with increasing PET percentages until the 40% replacement level, after which workability dropped. The PET-modified mixes obtained acceptable workability values for light to nominal reinforcement works except the 40% PET mix with a slump value of over 100 mm (ASTMC143/C143M-15a). True slumps were observed for all batches, indicating that PET's addition does not lead to collapse or early-age shear of concrete at all PET replacement levels. The increasing workability can be attributed to the reduced stiffness due to the low rates of water absorption by the PET plastic aggregates, leading to reduced bonding between the matrix and the PET aggregates. The early growth in workability contradicts workability results from past studies using PET in different ratios (Coppola et al., 2016; Ferreira et al., 2012; Ismail and AL-Hashmi, 2008; Lee et al., 2019; Rahmani et al., 2013; Silva et al., 2013). Nevertheless, these studies applied PET plastic flaked aggregates without heat pre-treatment. Slump results obtained by Islam et al. (2016), adopting a relatively similar PET pre-treatment (PET melted at 230 °C), conforms with the growing trend observed in this study. The compaction factor was relatively constant within the 10%- to 40%-PET modification levels and decreased with the 100% PET mix. However, a past study indicated a uniform increase in compaction factor with untreated PET plastic fine aggregate additions (Amalu et al., 2016).

#### 3.2. Mechanical properties

##### 3.2.1 Compressive strength tests

The compressive strength development at various curing ages for the varying percentages of PET additions are shown in Fig. 7. Steadily increase in compressive strength with curing age and decreased with

increasing PET percentages were observed. The PET-modified mix attained a compressive strength decrease up to 34.8% on the 28th day with the PET-100 mix. PET-modified mixes only achieved target compressive strength on the 7th day and failed to meet target compressive strength on the 14th and 28th day compared to the control mix. However, the 10%-, 20%-, 30%-, and 40%-PET batches achieved compressive strength requirement for M20 concrete grade in line with ASTM C39/C39M and are as such, suitable for mass concrete production. Generally, the decreasing trend noticed in this study conforms with several past studies utilizing PET as both fine and coarse aggregates (Akinyele and Ajede, 2018; Batayneh et al., 2007; Juki et al., 2013; Liu et al., 2015; Mohammed and Rahim, 2020; Mustafa et al., 2019; Saikia and De Brito, 2013; Saxena et al., 2018; Tang et al., 2020) Some of the reasons for the decreasing compressive strength with PET additions include: inhibition of the cement hydration reaction as a result of the PET aggregate's hydrophobia; reduced bonding strength between the cement matrix and the PET plastic aggregate surface (Gu and Ozbakkaloglu, 2016; Saikia and De Brito, 2012); the increased porosity and void content of PET-modified concrete; low water absorption; and low modulus of elasticity of PET aggregates compared to natural aggregates (Almeshal et al., 2020).

##### 3.2.2 Split tensile strength tests

The evolution of split tensile strength after 3, 7, 14, 21, and 28 days curing ages is illustrated in Fig. 8. Similar to compressive strength, split tensile strength steadily increased with curing age and gradually decreased with PET additions at all ages. After 3, 7, and 14 days for the 10%-PET-modified batch, early-age tensile strength values were slightly higher than that of the control batch (PET-00), as similar to a study by Needhidasan et al. (2020). This may be as a result of the reduced absorption offered by PET aggregate leading to increased cement hydration and tensile strength at the early age. Nonetheless, the results after 21, and 28 days showed a gain in strength for the PET-00 batch and slight declines with PET additions. The split tensile strength target of 2 N/mm<sup>2</sup> was achieved with all PET-modified batches after 21 days except the 100%-PET batch, indicating per ASTM C496/C496M-17 that they meet the recommended limits for mass concrete production.

The decreasing tensile strength noticed in this study conforms with numerous past studies utilizing PET as fine aggregates (Akinyele and Ajede, 2018; Batayneh et al., 2007; Choi et al., 2005; Galvão et al., 2011; Juki et al., 2013; Mohammed et al., 2019). Kou et al. (2009) attributed the decreasing split tensile strength to the smoother surface of the PET aggregates, the free-water accumulated by the PET particle at the interfacial transition zone (ITZ), and increased porosity (Albano et al., 2009; Kou et al., 2009).

#### 3.3. Microstructural analyses

##### 3.3.1 Scanning electron microscopy (SEM)

SEM experimentations were performed on the PET-10, PET-30, and PET-100 samples to obtain information on the effect of PET on the surface structure of the produced composites. The resultant microstructural graphs are presented in Fig. 9. The SEM analysis results showed a strong bond between the cement paste and the PET FA as seen in Fig. 9a with the least extent of honeycombing and micro pores. Fig. 9b highlights the formation of honeycombs and pore spaces with increasing PET-FA contents. The aggregates are seen clearly in Fig. 9c because of the more profound magnification degree indicating the formation of microcracks which further explains the decline in mechanical performance for the PET-100 mix batch.

##### 3.3.2 Energy-dispersive X-ray spectroscopy (EDX)

A visual analysis of the effect of PET on the surface structure of the produced composites has been done using the SEM analysis. Nevertheless, an EDX analysis was performed at selected areas on the PET-30

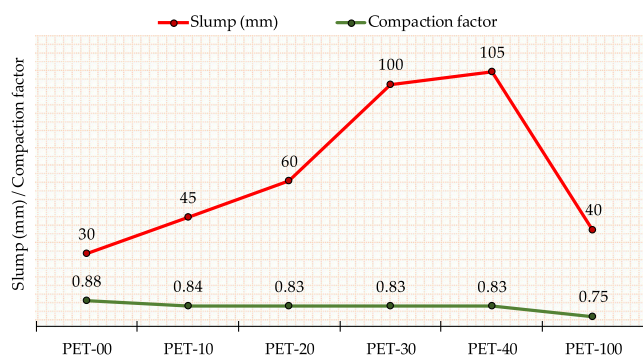


Fig. 6. Workability tests results.

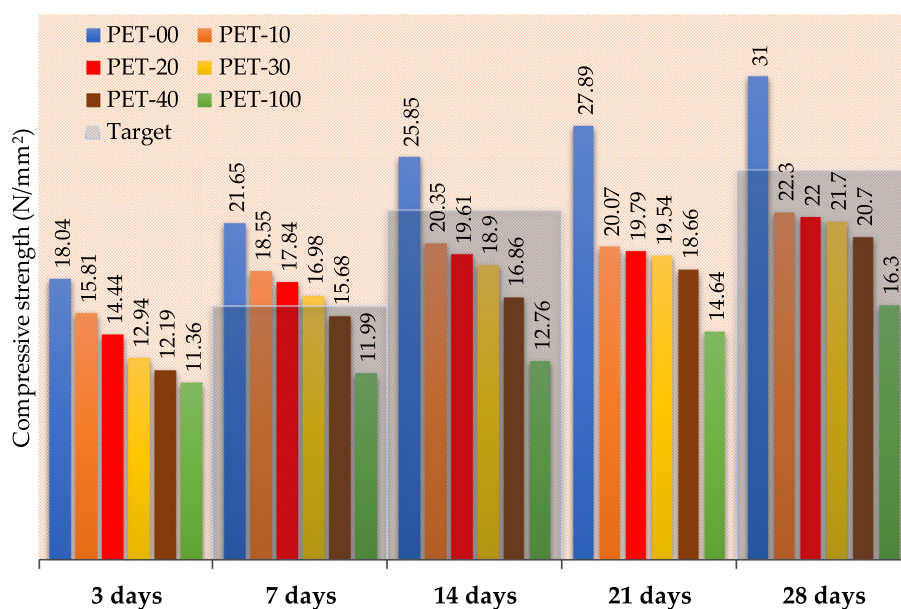


Fig. 7. Compressive strength tests results.

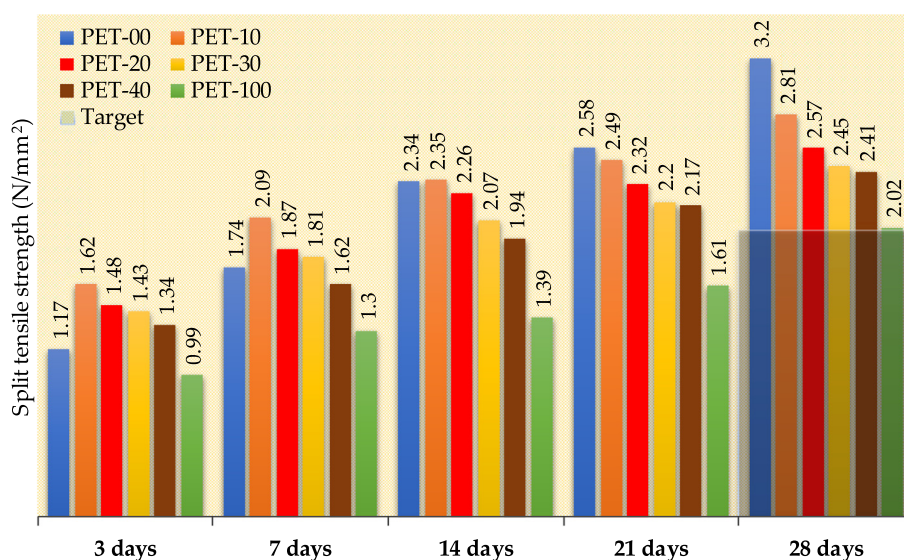


Fig. 8. Split tensile strength tests results.

and PET-100 samples shown in Fig. 9 to qualitatively and quantitatively evaluate the elemental composition of the composites. The EDX results and spectrum peaks are illustrated in Fig. 10. The EDX showed that individual samples' chemical compositions differ at multiple spots due to the varying emissions from the characteristic X-rays. EDX on the PET-30 indicated higher quantities of O and Ca, and trivial percentages of Mg, Si, C, Al, and Au. Whereas, PET-100 indicated the presence of only C, O, and Au, in order of magnitude as presented in Table 3. Showing a significant decrease in the bonding strength (absence of Ca) with PET additions.

### 3.4. Thermal analyses

#### 3.4.1 Differential scanning calorimetry (DSC)

A differential scanning calorimetry (DSC) was used to evaluate the temperature and heat flow through the PET-100 sample. The DSC result provides quantitative and qualitative data on the exothermic

and endothermic processes or heat capacity changes. The DSC scan result is illustrated in Fig. 11. The process began at 25 °C at a 10 °C per minute average heating rate. Through the process, a glass transition was observed with a start temperature of 63 °C and a midpoint  $T_g$  of 75 °C. An exothermic peak below decomposition temperature during heating was noticed at a temperature 199.88 °C; this can be due to the crystallization or curing of the PET within the sample. Correspondingly, a shift along the baseline was observed after the endothermic peak at 243.22°C; this can be ascribed to reasons like changes in either the sample's weight, the heating rate, or the sample's specific heat. Specific heat change can occur after the sample undergoes crystallization, curing, or melting (Shawe et al., 2000; TA Instruments, 2010).

#### 3.4.2 Thermogravimetric analysis (TGA)

The TGA was performed to measure the rate at which the 100%PET-modified sample's mass changes with varying temperatures. The TGA

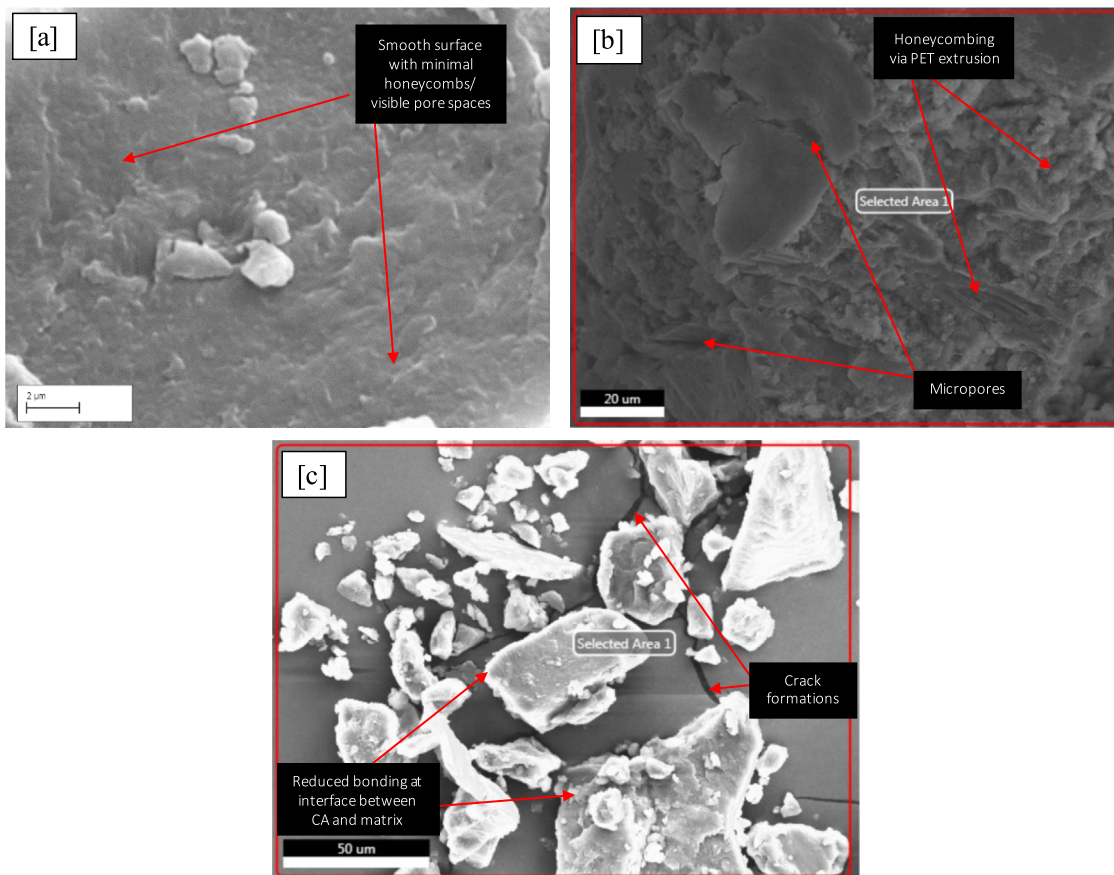


Fig. 9. SEM micrographs [a] PET-10 [b] PET-30 [c] PET-100.

scan result is shown in Fig. 12. A 10.5 mg sample was tested at a heating rate of 5 °C/min, the initial temperature at the start of the process was 29.87 °C, and the final temperature was 644.36 °C. Generally, there was a continuous weight loss with increasing temperature. The sample underwent dual-stage decomposition. The first stage had an onset temperature of 380 °C, midpoint of 420 °C, an offset temperature of 360 °C, accounting for an 87.41% reduction in sample mass. The second stage indicated an onset temperature of 520 °C, an offset temperature of 537 °C, and accounted for a further mass loss of 12.79%. The first stage of the weight loss can be related to the molecular fragmentation of the polymer and the evaporation of free water molecules within and around the composite, while the second stage may be a result of the in-situ formation of metallic oxides during the decomposition.

#### 4. Correlation and regressions

Bivariate correlation analyses were performed to determine whether relationships exist between the workability and mechanical parameters assessed in this study, including PET %, slump, compaction factor, split tensile strength, and compressive strength. The coefficients of correlation are presented in Table 4. PET % showed significant negative correlations with compressive strength ( $r = -0.665$ ), split tensile strength ( $r = 0.507$ ), and compaction factor ( $r = -0.966$ ), and an insignificant correlation with slump ( $r = -0.032$ ). Compressive strength similarly showed a high positive correlation with split tensile strength ( $r = 0.870$ ) and compaction factor ( $r = -0.839$ ), and significant negative correlations with slump ( $r = -0.559$ ). The correlations established in these analyses do not infer cause and effect relationships. Nevertheless, they explain the degree of inter-relations between these parameters.

A series of bivariate regression analyses were further done to recognize the interdependencies (cause and effect relationships) amongst

the mechanical and workability parameters evaluated based on the PET modification. The datasets were firstly examined with a box plot, and there were few outliers noticed in the measured values for compressive and split tensile strength. The values of each criterion variable were evaluated using a test of normality utilizing Shapiro-Wilk ( $p > 0.05$ ); for all three variable datasets a normal distribution was observed. Based on Levene's test of equality, there was no violation of homogeneity of variance. From the one-way ANOVA on the compressive strength data ( $F(5,24) = 6.495, p < .001$ ), and the split tensile strength ( $F(5,24) = 1.735, p = .165$ ) there were statistically significant differences between their means. A Tukey post hoc test indicated that the compressive strength was statistically significantly lower after taking the PET-100 ( $13.41 \pm 2.0 \text{ min}, p < .001$ ) compared to the PET-00 ( $24.88 \pm 5.1 \text{ min}, p < .001$ ).

The trend functions and mathematical models from the regression of the measured parameters are shown in Fig. 13; non-statistically significant linear functions were established with PET% as a predictor for compressive strength ( $C_s$ ) ( $R^2 = 0.4418$ ) and split tensile strength ( $S_s^t$ ) ( $R^2 = 0.2568$ ). At the same time, highly statistically dependent linear functions were obtained for compaction factor ( $W_{CF}$ ) against PET % ( $R^2 = 0.933$ ) and for split tensile strength against compressive strength ( $R^2 = 0.7569$ ). Also, a polynomial function was obtained for the slump ( $W_{SI}$ ) against PET % ( $R^2 = 0.9236$ ). A summary of the regressions is presented in Table 5.

#### 5. Cost analysis

This study evaluated the economic, mechanical, microstructural, and thermal properties of concrete containing waste PET as fine aggregates. The result of the empirical cost evaluation of PET/Fine aggregates mix as shown in Table 6 revealed that

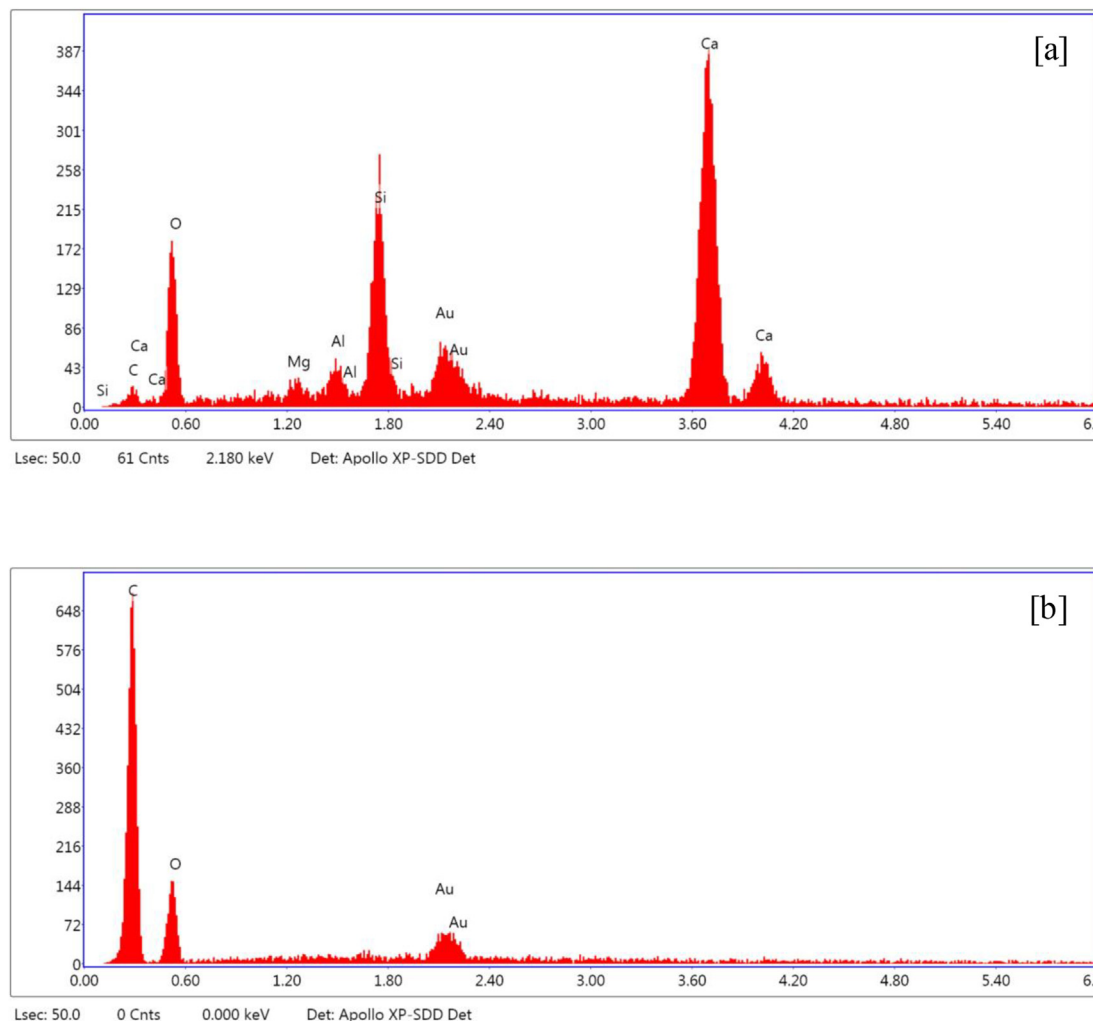


Fig. 10. EDX spectrums [a] PET-30 [b] PET-100.

Table 3  
EDX Smart Quant elemental intensity results.

PET-30							
Element	C	O	Mg	Al	Si	Au	Ca
Atomic %	6.99	57.97	0.82	1.38	8.51	0.70	23.63
Weight %	3.51	38.77	0.84	1.56	10.00	5.74	39.59
PET-100							
Element	C	O	Au	-	-	-	-
Atomic %	76.10	23.53	0.37	-	-	-	-
Weight %	67.04	27.62	5.34	-	-	-	-

increasing cost and proportion of PET was negatively and significantly related to concrete compressive strength at 1 percent significance level for the 3-Days and 7-Days test and 5 percent significance level for the 14, 21 and 28 -Days test respectively. This implies that the increasing cost of PET is not economically recommendable in relation to fine aggregates. Deeper insight from the result suggests that despite increases in PET cost, comprehensive of the concrete revealed retardation of 0.025, 0.990, 0.961, and 0.949, 0.946 N/mm<sup>2</sup> for the 3, 7, 14, 21, and 28-

days respective testing periods. The compaction factor averagely reduces by more than proportionate magnitude value -1.732.

However, the slump test suggests a significant increase by 0.960 mm following increases in PET costs. Thus more fine aggregates support compressive strength and compaction factor of concretes while slump test requires more of PET, as shown by the workability test analysis.

Also, the average split (Table 7) tensile strength follows the same negative trend for the cost of PET at 0.982, 0.980, 0.992, and



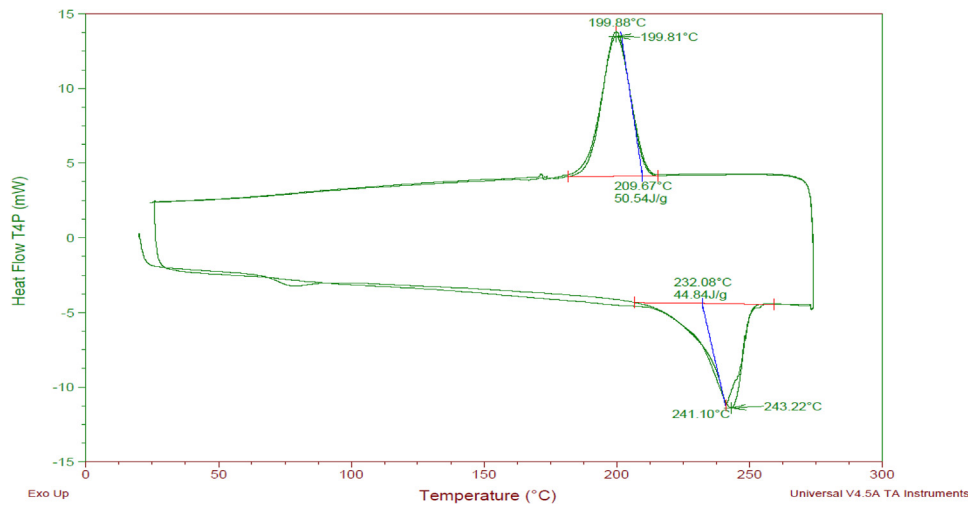


Fig. 11. DSC scan on PET-100.

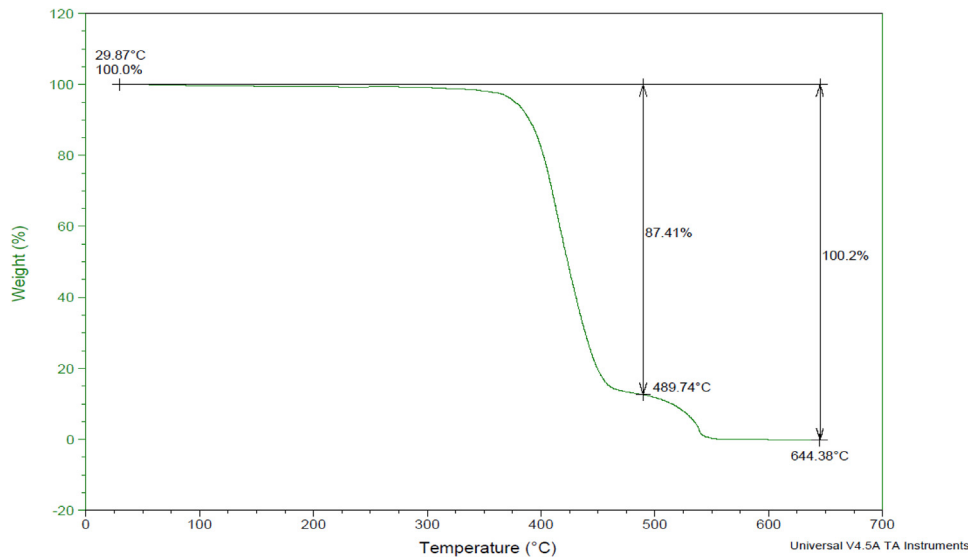


Fig. 12. TGA graph of the PET-100 sample.

Table 4  
Correlation coefficient matrix.

Parameters	Compressive strength	Split tensile strength	Slump value	Compaction factor
PET %	-0.665**	-0.507**	0.032	-0.966**
Compressive strength	1	0.870**	-0.559	0.839*
Split tensile strength		1	0.319	0.464
Slump value			1	-0.022
Compaction factor				1

\*\* Correlation is significant at the 0.01 level (2-tailed).

\* Correlation is significant at the 0.05 level (2-tailed).

0.947 N/mm<sup>2</sup>. Therefore, it could be seen that fine aggregates yield better economic outcomes in relation to the compressive strength and compaction factor of the concretes. At the same time, the cost of PET appears more economical and cost-effective for the slump testing approach.

The credibility of the estimated models (F-statistics) were confirmed at 1 percent significance level, and its explanatory strength (R-Squared) with a minimum value of 60 percent for the compaction factor.

## 6. Conclusions

This study evaluated the effects of recycling waste PET plastic bottles as a full or partial substitute for fine natural aggregates on the workability, mechanical, microstructural, economic, and thermal properties of concrete. The following conclusions are drawn based on the results obtained from the laboratory tests:

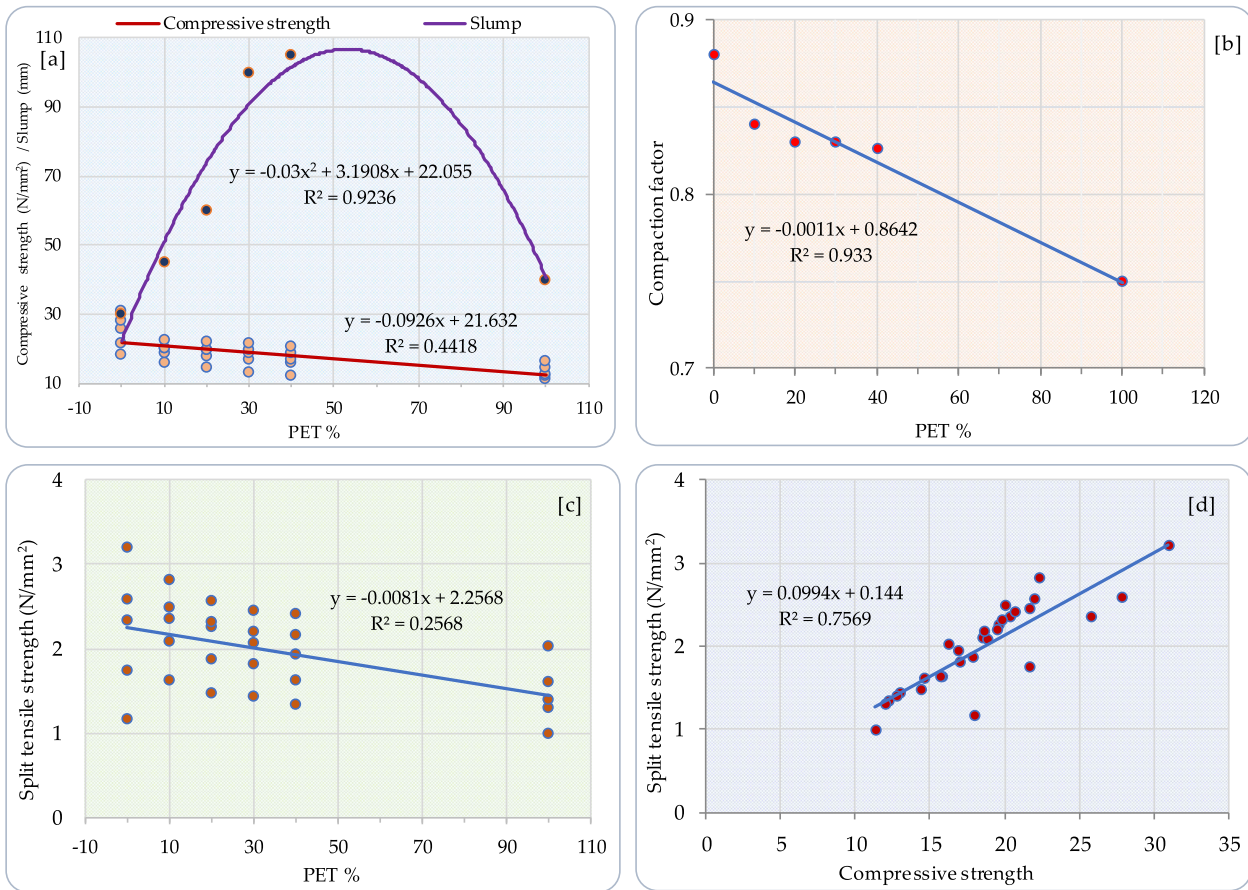


Fig. 13. Relationships between (A) Slump/Compressive strength and PET % (B) compaction factor and PET % (C) split tensile strength and PET% (D) split tensile strength and compressive strength.

Table 5  
Summary of regression.

Variables		Model	Statistical Coefficients		
Criterion	Predictor		Mean	Std. dev.	R <sup>2</sup>
$W_{Sl}$	PET%	$W_{Sl} = -0.03(PET\%)^2 + 3.1908(PET\%) + 0.9236$	63.33	1.030	0.9236
$W_{CF}$	PET%	$W_{CF} = -0.0011(PET\%) + 0.8642$	0.826	0.041	0.933
$C_S$	PET%	$C_S = -0.0926(PET\%) + 21.632$	18.546	3.059	0.442
$S_S^c$	PET%	$S_S^c = -0.0081(PET\%) + 2.2568$	1.988	0.266	0.2568
$S_S^t$	$C_S$	$S_S^t = 0.0994(C_S) + 0.144$	1.988	0.526	0.757

Table 6  
Compressive strength cost analysis.

Cost Analysis	Compressive Strength Analysis					Workability Test Analysis	
	3-Days	7- Days	14-Days	21 Days	28-Days	Slump	Compaction Factor
Predictors Mix Proportion: PET /Granite costs							
Constant	16.935***	19.630***	21.725***	20.635***	22.930***	22.500	0.840***
Coefficients	-0.025***	-0.990***	-0.961**	-0.949**	-0.946**	0.960**	-1.732
R-squared	0.983	0.980	0.924	0.900	0.896	0.922	0.600
Adjusted R	0.974	0.970	0.886	0.850	0.843	0.883	0.400
F-Statistics	113.314***	98.302***	24.271**	17.955**	17.165**	23.610**	3.000

Note: \*\*\*, \*\* represents significance at 1% and 10% level.

**Table 7**  
Split Tensile strength cost-effect.

Cost Analysis	Split Tensile strength				
	Predictors Proportion Mix: PET /Granite costs	3-Days	7- Days	14-Days	21 Days
Constant	1.690***	2.215***	2.510***	2.565***	33.238***
Coefficients	-0.982**	-0.980**	-0.992***	-0.960**	-0.947**
R-squared	0.964	0.961	0.984	0.921	0.896
Adjusted R	0.946	0.941	0.975	0.882	0.844
F-Statistics	53.884**	48.779**	120.024***	23.422**	17.286**

Note: \*\*\*, \*\* represents significance at 1% and 10% level.

- i. The workability of the fresh-mix concrete increases with increasing the percentages of waste PET plastics until the 40% PET level, beyond which workability declines. Nonetheless, all PET batches attained workability values suitable for low to nominal reinforcement works.
- ii. As the curing age of concrete increased, the compressive strength increased but then decreased with increasing percentages of waste PET plastics after 3, 7, 14, 21, and 28 days of curing. The modified PET mixes unable to attain the target design strength for grade M25 concrete after 28 days. However, 10% to 40% of PET-modified mixes attained suitable strength for grade M20 concrete.
- iii. Split tensile strength increased steadily with curing age and decreased with PET additions. PET modification resulted in early tensile strength gain compared to the control mix. It should be noted that all PET-modified mixes reached the recommended threshold specified for split tensile strength after 28 days.
- iv. PET% showed significant negative correlations with compressive strength ( $r = -0.665$ ), split tensile strength ( $r = -0.507$ ), and compaction factor ( $r = -0.966$ ), and an insignificant correlation with slump ( $r = -0.032$ ), compressive strength similarly showed a high positive correlation with split tensile strength ( $r = 0.870$ ). Regression analysis indicated statistically significant linear and polynomial dependencies between the parameters; hence multiple variations were established.
- v. EDX on the PET-30 indicated higher quantities of O and Ca, and trival percentages of Mg, Si, C, Al, and Au. Whereas PET-100 indicated the presence of only C, O, and Au.
- vi. The DSC scan indicated that the 100%PET sample endured three transition stages. A glass transition with an onset temperature of 63 °C and a midpoint  $T_g$  of 75 °C, an exothermic peak below decomposition temperature during cooling was noticed at a temperature of 199.88 °C from the crystallization of the PET in the sample, and a baseline shift after the endothermic peak at 243.22°C during the heating process.
- vii. TGA scan showed that the 100%PET sample suffered dual-stage decomposition. The initial stage had an onset temperature of 380 °C, midpoint of 420 °C, an offset temperature of 360 °C, accounting for an 87.41% reduction in sample mass, while the final stage indicated an onset temperature of 520 °C, an offset temperature of 537 °C and accounted for a further mass loss of 12.79%.
- viii. The cost of PET appears more economical and cost-effective for the slump testing approach, while fine aggregates yield better economic outcomes in relation to the compressive strength.

## Declaration of Competing Interest

The authors declare that they have no known competing financial interests or personal relationships that could have appeared to influence the work reported in this paper.

## Acknowledgement

The authors wish to thank the chancellor and Covenant University management for the platform made available for this research work. The authors also appreciate the Experimental Techniques Centre (ETC) Brunel University London for the platform made available for performing Microstructural and Thermal Analyses of samples.

## References

- Akçaözöglü, S., Atiş, C.D., Akçaözöglü, K., 2010. An investigation on the use of shredded waste PET bottles as aggregate in lightweight concrete. *Waste Manag.* 30 (2), 285–290. <https://doi.org/10.1016/j.wasman.2009.09.033>.
- Akinyele, J.O., Ajede, A., 2018. The use of granulated plastic waste in structural concrete. *African J. Sci. Technol. Innov. Dev.* 10 (2), 169–175. <https://doi.org/10.1080/20421338.2017.1414111>.
- Albano, C., Camacho, N., Hernández, M., Matheus, A., Gutiérrez, A., 2009. Influence of content and particle size of waste pet bottles on concrete behavior at different w/c ratios. *Waste Manag.* 29 (10), 2707–2716. <https://doi.org/10.1016/j.wasman.2009.05.007>.
- Almeshal, I., Tayeh, B.A., Alyousef, R., Alabduljabbar, H., Mustafa Mohamed, A., Alaskar, A., 2020. Use of recycled plastic as fine aggregate in cementitious composites: A review. *Constr. Build. Mater.* 253, 119146. <https://doi.org/10.1016/j.conbuildmat.2020.119146>.
- Amalu, R., Azeef, A., Muhammad, H., Rejith, K., Vijitha, V., 2016. Use of Waste Plastic as Fine Aggregate Substitute in Concrete. *Int. J. Sci. Eng. Res.* 7.
- An, M., Huang, H., Wang, Y., Zhao, G., 2020. Effect of thermal cycling on the properties of high-performance concrete: Microstructure and mechanism. *Constr. Build. Mater.* 243, 118310. <https://doi.org/10.1016/j.conbuildmat.2020.118310>.
- ASTM C143/C143M-15a, 2015. Standard Test Method for Slump of Hydraulic-Cement Concrete. West Conshohocken, PA. [https://doi.org/10.1520/C0143\\_C0143M-15A](https://doi.org/10.1520/C0143_C0143M-15A).
- ASTM C496/C496M-17, 2017. Standard Test Method for Splitting Tensile Strength of Cylindrical Concrete Specimens. [https://doi.org/10.1520/C0496\\_C0496M-17](https://doi.org/10.1520/C0496_C0496M-17).
- ASTM E2160-04, 2018. Standard Test Method for Heat of Reaction of Thermally Reactive Materials by Differential Scanning Calorimetry. West Conshohocken, PA. <https://doi.org/10.1520/E2160-04R18>.
- Babafemi, Adewumi, Šavija, Branko, Paul, Svavsh, Anggraini, Vivi, 2018. Engineering properties of concrete with waste recycled plastic: A review. *Sustain* 10 (11), 3875. <https://doi.org/10.3390/su10113875>.
- Bamigboye, Gideon O., Bassey, Daniel E., Olukanni, David O., Ngene, Ben U., Adegoke, Dunmininu, Odetoyan, Abimbola O., Kareem, Mutiu A., Enabulele, David O., Nworgu, Austin T., 2020. Waste materials in highway applications: An overview on generation and utilization implications on sustainability. *J. Clean. Prod.* 283, 124581. <https://doi.org/10.1016/j.jclepro.2020.124581>.
- Bamigboye, G.O., Ngene, B.U., Ademola, D., Jolayemi, J.K., 2019. Experimental Study on the Use of Waste Polyethylene Terephthalate (PET) and River Sand in Roof Tile Production. *J. Phys. Conf. Ser.* 1378, 042105. <https://doi.org/10.1088/1742-6596/1378/4/042105>.

- Batayneh, Malek, Marie, Iqbal, Asi, Ibrahim, 2007. Use of selected waste materials in concrete mixes. *Waste Manag.* 27 (12), 1870–1876. <https://doi.org/10.1016/j.wasman.2006.07.026>.
- Bhardwaj, Bavita, Kumar, Pardeep, 2017. Waste foundry sand in concrete: A review. *Constr. Build. Mater.* 156, 661–674. <https://doi.org/10.1016/j.conbuildmat.2017.09.010>.
- Boucedra, Aissa, Bederina, Madani, Ghernouti, Youcef, 2020. Study of the acoustical and thermo-mechanical properties of dune and river sand concretes containing recycled plastic aggregates. *Constr. Build. Mater.* 256, 119447. <https://doi.org/10.1016/j.conbuildmat.2020.119447>.
- Choi, Yun-Wang, Moon, Dae-Joong, Chung, Jee-Seung, Cho, Sun-Kyu, 2005. Effects of waste PET bottles aggregate on the properties of concrete. *Cem. Concr. Res.* 35 (4), 776–781. <https://doi.org/10.1016/j.cemconres.2004.05.014>.
- Colangelo, F., Cioffi, R., Liguori, B., Iucolano, F., 2016. Recycled polyolefins waste as aggregates for lightweight concrete. *Compos. Part B Eng.* 106, 234–241. <https://doi.org/10.1016/j.compositesb.2016.09.041>.
- Coppola, B., Courard, L., Michel, F., Incarnato, L., Di Maio, L., 2016. Investigation on the use of foamed plastic waste as natural aggregates replacement in lightweight mortar. *Compos. Part B Eng.* 99, 75–83. <https://doi.org/10.1016/j.compositesb.2016.05.058>.
- Faraj, Rabar H., Hama Ali, Hunar F., Sherwani, Aryan Far H., Hassan, Bedar R., Karim, Hogr, 2020. Use of recycled plastic in self-compacting concrete: A comprehensive review on fresh and mechanical properties. *J. Build. Eng.* 30, 101283. <https://doi.org/10.1016/j.jobe.2020.101283>.
- Faraj, Rabar H., Sherwani, Aryan Far H., Daraei, Ako, 2019. Mechanical, fracture and durability properties of self-compacting high strength concrete containing recycled polypropylene plastic particles. *J. Build. Eng.* 25, 100808. <https://doi.org/10.1016/j.jobe.2019.100808>.
- Ferreira, L., De Brito, J., Saikia, N., 2012. Influence of curing conditions on the mechanical performance of concrete containing recycled plastic aggregate. *Constr. Build. Mater.* 36, 196–204. <https://doi.org/10.1016/j.conbuildmat.2012.02.098>.
- Galvão, José Carlos Alves, Portella, Kleber Franke, Joukoski, Alex, Mendes, Roberto, Ferreira, Elizeu Santos, 2011. Use of waste polymers in concrete for repair of dam hydraulic surfaces. *Constr. Build. Mater.* 25 (2), 1049–1055. <https://doi.org/10.1016/j.conbuildmat.2010.06.073>.
- Goldstein, J.I., Newbury, D.E., Michael, J.R., Ritchie, N.W.M., Scott, J.H.J., Joy, D.C., 2018. *Scanning Electron Microscopy and X-Ray Microanalysis*. Springer. <https://doi.org/10.1007/978-1-4939-6676-9>.
- Groenewoud, W.M., 2001. Thermogravimetry. In: *Characterisation of Polymers by Thermal Analysis*. Elsevier, pp. 61–76. <https://doi.org/10.1016/B978-044450604-7/50003-0>.
- Gu, Lei, Ozbakkaloglu, Togay, 2016. Use of recycled plastics in concrete: A critical review. *Waste Manag.* 51, 19–42. <https://doi.org/10.1016/j.wasman.2016.03.005>.
- Islam, M.J., Meherier, M.S., Islam, A.K.M.R., 2016. Effects of waste PET as coarse aggregate on the fresh and hardened properties of concrete. *Constr. Build. Mater.* 125, 946–951. <https://doi.org/10.1016/j.conbuildmat.2016.08.128>.
- Ismail, Z.Z., AL-Hashmi, E.A., 2008. Use of waste plastic in concrete mixture as aggregate replacement. *Waste Manag.* 28, 2041–2047. <https://doi.org/10.1016/j.wasman.2007.08.023>.
- Jeske, H., Schirp, A., Cornelius, F., 2012. Development of a thermogravimetric analysis (TGA) method for quantitative analysis of wood flour and polypropylene in wood plastic composites (WPC). *Thermochim. Acta* 543, 165–171. <https://doi.org/10.1016/j.tca.2012.05.016>.
- Juki, Mohd Irwan, Awang, Mazni, Annas, Mahamad Mohd Khairil, Boon, Koh Heng, Othman, Norzila, binti Abdul Kadir, Aeslina, Roslan, Muhammad Asyraf, Khalid, Faisal Sheikh, 2013. Relationship between compressive, splitting tensile and flexural strength of concrete containing granulated waste polyethylene terephthalate (PET) bottles as fine aggregate. *Adv. Mater. Res.* 795, 356–359. <https://doi.org/10.4028/www.scientific.net/AMR.795.356>.
- Kou, S.C., Lee, G., Poon, C.S., Lai, W.L., 2009. Properties of lightweight aggregate concrete prepared with PVC granules derived from scraped PVC pipes. *Waste Manag.* 29 (2), 621–628. <https://doi.org/10.1016/j.wasman.2008.06.014>.
- Lee, Zoe Harmonie, Paul, Suvash Chandra, Kong, Sih Ying, Susilawati, Susilawati, Yang, Xu, 2019. Modification of Waste Aggregate PET for Improving the Concrete Properties. *Adv. Civ. Eng.* 2019, 1–10. <https://doi.org/10.1155/2019/6942052>.
- Li, Xuemiao, Ling, Tung-Chai, Hung Mo, Kim, 2020. Functions and impacts of plastic/rubber wastes as eco-friendly aggregate in concrete – A review. *Constr. Build. Mater.* 240, 117869. <https://doi.org/10.1016/j.conbuildmat.2019.117869>.
- Liu, Feng, Yan, Yong, Li, Lijuan, Lan, Cheng, Chen, Gongfa, 2015. Performance of recycled plastic-based concrete. *J. Mater. Civ. Eng.* 27 (2). [https://doi.org/10.1061/\(ASCE\)MT.1943-5533.0000989](https://doi.org/10.1061/(ASCE)MT.1943-5533.0000989).
- Maharaj, Rean, Maharaj, Chris, Mahase, Martina, 2019. The performance and durability of polyethylene terephthalate and crumb rubber-modified road pavement surfaces. *Prog. Rubber Plast. Recycl. Technol.* 35 (1), 3–22. <https://doi.org/10.1177/1477760618798425>.
- Mohammed, A.A., Mohammed, I.I., Mohammed, S.A., 2019. Some properties of concrete with plastic aggregate derived from shredded PVC sheets. *Constr. Build. Mater.* 201, 232–245. <https://doi.org/10.1016/j.conbuildmat.2018.12.145>.
- Mohammed, Azad A., Rahim, Aso A. Faqe, 2020. Experimental behavior and analysis of high strength concrete beams reinforced with PET waste fiber. *Constr. Build. Mater.* 244, 118350. <https://doi.org/10.1016/j.conbuildmat.2020.118350>.
- Mustafa, M.A.T., Hanafi, I., Mahmoud, R., Tayeh, B.A., 2019. Effect of partial replacement of sand by plastic waste on impact resistance of concrete: experiment and simulation. *Structures* 20, 519–526. <https://doi.org/10.1016/j.istruc.2019.06.008>.
- Needhidasan, S., Ramesh, B., Joshua Richard Prabu, S., 2020. Experimental study on use of E-waste plastics as coarse aggregate in concrete with manufactured sand. *Mater. Today: Proc.* 22, 715–721. <https://doi.org/10.1016/j.matpr.2019.10.006>.
- Perera, S., Arulrajah, A., Wong, Y.C., Horpibulsuk, S., Maghool, F., 2019. Utilizing recycled PET blends with demolition wastes as construction materials. *Constr. Build. Mater.* 221, 200–209. <https://doi.org/10.1016/j.conbuildmat.2019.06.047>.
- Rahmani, E., Dehestani, M., Beygi, M.H.A., Allahyari, H., Nikbin, I.M., 2013. On the mechanical properties of concrete containing waste PET particles. *Constr. Build. Mater.* 47, 1302–1308. <https://doi.org/10.1016/j.conbuildmat.2013.06.041>.
- Sadrmoontazi, A., Dolati-Milehsara, S., Lotfi-Omran, O., Sadeghi-Nik, A., 2016. The combined effects of waste Polyethylene Terephthalate (PET) particles and pozzolanic materials on the properties of self-compacting concrete. *J. Clean. Prod.* 112, 2363–2373. <https://doi.org/10.1016/j.jclepro.2015.09.107>.
- Saikia, N., De Brito, J., 2013. Waste polyethylene terephthalate as an aggregate in concrete. *Mater. Res.* 16, 341–350. <https://doi.org/10.1590/S1516-14392013005000017>.
- Saikia, Nabajyoti, de Brito, Jorge, 2012. Use of plastic waste as aggregate in cement mortar and concrete preparation: A review. *Constr. Build. Mater.* 34, 385–401. <https://doi.org/10.1016/j.conbuildmat.2012.02.066>.
- Saxena, R., Siddique, S., Gupta, T., Sharma, R.K., Chaudhary, S., 2018. Impact resistance and energy absorption capacity of concrete containing plastic waste. *Constr. Build. Mater.* 176, 415–421. <https://doi.org/10.1016/j.conbuildmat.2018.05.019>.
- Sharma, Raju, Bansal, Prem Pal, 2016. Use of different forms of waste plastic in concrete - A review. *J. Clean. Prod.* 112, 473–482. <https://doi.org/10.1016/j.jclepro.2015.08.042>.
- Shawe, J., Riesen, R., Widmann, J., Schubnell, M., 2000. Interpreting DSC curves Part 1: Dynamic measurements, Information for users of METTLER TOLEDO thermal analysis systems.
- Silva, R.V., de Brito, J., Saikia, Nabajyoti, 2013. Influence of curing conditions on the durability-related performance of concrete made with selected plastic waste aggregates. *Cem. Concr. Compos.* 35 (1), 23–31. <https://doi.org/10.1016/j.cemconcomp.2012.08.017>.
- Spiesz, P., Rouvas, S., Brouwers, H.J.H., 2016. Utilization of waste glass in translucent and photocatalytic concrete. *Constr. Build. Mater.* 128, 436–448. <https://doi.org/10.1016/j.conbuildmat.2016.10.063>.
- TA Instruments, 2010. *Interpreting Unexpected Events and Transitions in DSC Results*, TA039.
- Tang, Z., Li, W., Ke, G., Zhou, J.L., Tam, V.W.Y., 2019. Sulfate attack resistance of sustainable concrete incorporating various industrial solid wastes. *J. Clean. Prod.* 218, 810–822. <https://doi.org/10.1016/J.JCLEPRO.2019.01.337>.
- Tang, Zhuo, Li, Wengui, Tam, Vivian W.Y., Xue, Caihong, 2020. Advanced progress in recycling municipal and construction solid wastes for manufacturing sustainable construction materials. *Resour. Conserv. Recycl.* X 6, 100036. <https://doi.org/10.1016/j.rcrx.2020.100036>.
- UNEP, 2018. *Single-Use Plastic: A Roadmap for Sustainability*, United Nation Environment Programme.
- US Environmental Protection Agency (EPA), 2017. *Advancing Sustainable Materials Management: 2017 Fact Sheet*. <https://doi.org/10.1017/CBO9781107415324.004>.